Host-Guest Induced Electron Transfer Triggers Radical-Cation Catalysis

Rebecca L. Spicer,[†] Athanasios D. Stergiou, [§] Tom A. Young, [‡] Fernanda Duarte,[‡,*] Mark D. Symes[§,*] and Paul J. Lusby[†,*]

[†] EaStCHEM School of Chemistry, University of Edinburgh, Joseph Black Building, David Brewster Road, Edinburgh, Scotland, EH9 3FJ, U.K.

[§] WestCHEM, School of Chemistry, University of Glasgow, University Avenue, Glasgow G12 8QQ, U.K.

[‡] Chemistry Research Laboratory, University of Oxford, Mansfield Road, Oxford, OX1 3TA, U.K.

Supporting Information Placeholder

ABSTRACT: Modifying the reactivity of substrates by encapsulation is a fundamental principle of capsule catalysis. Here we show an alternative strategy, wherein catalytic activation of otherwise inactive quinone "co-factors" by a simple Pd_2L_4 capsule promotes a range of bulk-phase, radical-cation cycloadditions. Solution electron transfer experiments and cyclic voltammetry show the cage anodically shifts the redox potential of the encapsulated quinone by a significant 1 V. Moreover, the capsule also protects the reduced semiquinone from protonation, thus transforming the role of quinones from stoichiometric oxidants into catalytic single electron acceptors. We envisage that the host-guest induced release of an "electron hole" will translate to various forms of non-encapsulated catalysis that involve other difficult to handle, highly reactive species.

The modulation of reactivity using transition state-stabilizing interactions is the dominant mechanism that enzymes employ to achieve incredible rate enhancements.[1] Their remarkable activity has inspired a generation of scientists to create artificial mimics using hollow, substrate-binding constructs.[2] Enzymes, however, do not only change the reactivity of bound substrates but also other species, such as co-factors, which are essential for catalytic activity. The use of encapsulated transition metal catalysts,[3] as exemplified by Toste, Raymond and Bergman,[4] can be viewed as a form of biomimetic holocatalysis. Whilst common in nature, manipulation of redox properties using synthetic hosts is much less common,[5] even less so for catalytic applications.[6] Herein we show that the binding of several commercially available quinones by a simple coordination cage generates catalytic activity not inherent in either component.

We have previously shown that cages **C-1** and **C-2** (Scheme 1) bind and activate quinones,[7a] facilitating Diels–Alder (DA) catalysis.[2h] As activation results from a lowered LUMO,[7b] we expected that encapsulation would increase the quinone redox potential, triggering electron transfer (ET) from a free substrate and thus generating bulk-phase radical-cation reactivity (Scheme 1a,b). This mode of cage catalysis complements usual forms that involve substrate encapsulation;[2] it allows a wider, size-independent reactant scope and avoids product inhibition[2b,c] yet cannot easily facilitate the types of selectivity attainable using confinement effects. We were also expectant that the cage could transform the intrinsic role of quinones from stoichiometric $2(H^+ + e^-)$ oxidants to catalytic *one-electron* acceptors because the poly-cationic shell should "protect" the semiquinone radical-anion from protonation. This fundamental switch in reactivity would make it distinct from small molecule non-covalent activation of *o*-quinones.[8]

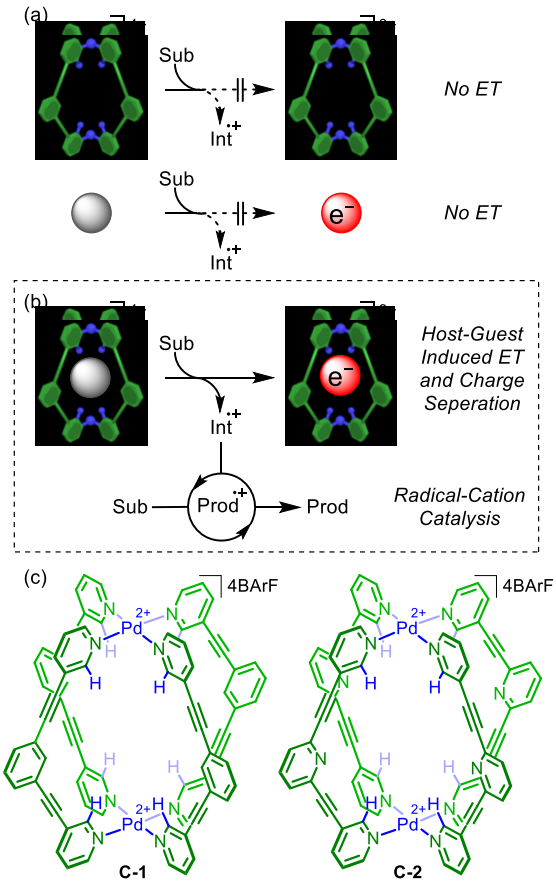

Scheme 1. Supramolecular redox catalysis. (a) Cage and "co-factor" are separately inactive but (b) encapsulation switches on electron transfer (ET) and radical-cation reactivity. (c) Chemical structure of cages **C-1** and **C-2** used in this study.

Initial catalytic studies focused on the electron rich alkene *trans*-anethole, a substrate that Bauld has shown undergoes radical cation cyclizations induced by the single electron oxidant, the Ledwith-Weitz salt.[9a,b] Selecting fluoranil, **Q-1**, because it is both a mild oxidant and a guest for **C-1** (K_a = 120 M^{-1}; see Supporting Information), we found that neither species separately show any reactivity towards this substrate. However, combining **C-1** and **Q-1** (5 mol% each) gave rapid formation (< 1 h) of the [2+2] homodimer **1**, albeit in only 34% yield (Scheme 2b) alongside unreacted starting material. Yoon has suggested that the homodimer undergoes facile retrocycloaddition,[10a] explaining this poor conversion. Pleasingly, the [4+2] cycloaddition reaction of *trans*-anethole and cyclopentadiene showed full consumption of the limiting reactant giving cycloadduct **2** in an excellent 99% yield (Scheme 2a; Table 1, entry 1). The diastereoselectivity of product **2** is the same within error of that observed by Bauld (83:17 vs 85:15)[9c] suggesting a common radical cation reaction manifold.

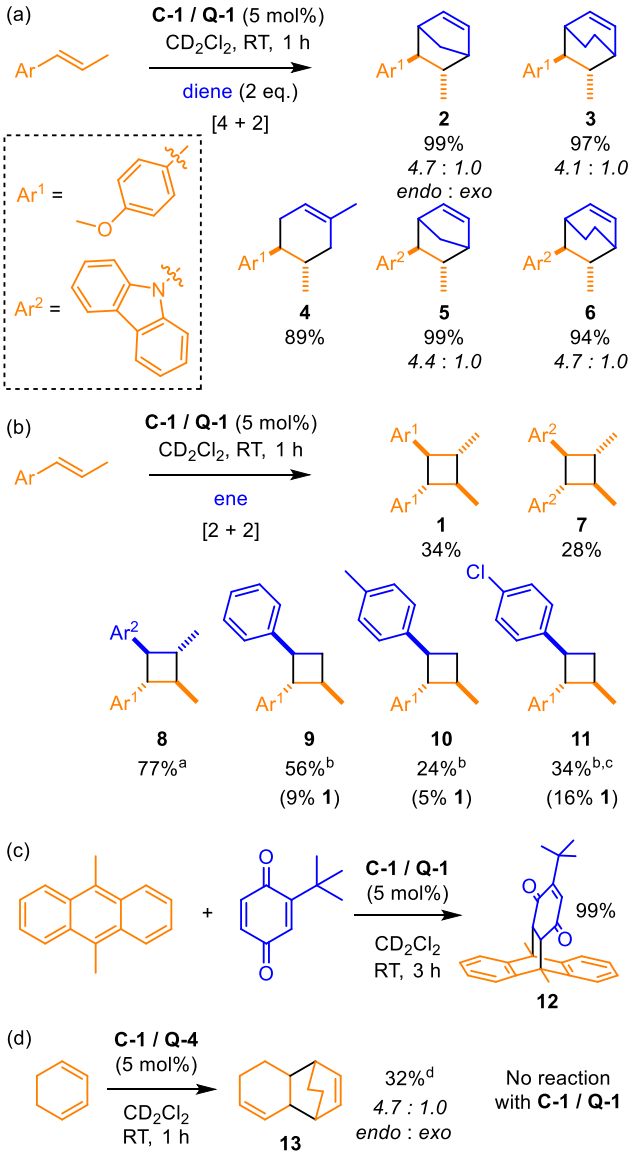

Scheme 2. Cage-quinone catalyzed [4+2] and [2+2] cycloaddition reactions. Yields determined by ^{1}H NMR spectroscopy. [a]1 eq. Ar^2, 5 eq Ar^1. [b]10 eq. styrene derivative. [c]Yield at 24 h. [d]61% cyclohexadiene unreacted.

Control reactions again show that neither **Q-1** nor **C-1** separately give cycloadduct **2** (Table 1, entries 2 and 3). Adding the competitive inhibitor anthraquinone **Q-10** (K_a = 5 × 10^7 M^{-1}) also completely curtails reactivity (Table 1, entry 4). This shows that formation of the **Q-1⊂C-1** host-guest complex is key. We have also investigated the possibility of hidden Brønsted acid catalysis by reacting the substrates with 10 mol% hydronium BArF. This reaction shows minimal consumption of substrates after 1 h and even after 24 h shows no obvious formation of compound **2** (see Figure S10). In contrast, **Q-1⊂C-1** gives quantitative yield of **2** in 1 h. The diversity of encapsulated *p*-quinones used to effect cycloaddition has also been investigated.[11] Tetrahalogenated quinones **Q-2** and **Q-3** both gave the cycloadduct in close to quantitative yield, as did DDQ, **Q-4**, (Table 1, entries 6–8). Interestingly, the *endo*:*exo* ratio with **Q-4** (3.6:1) was different from that obtained with **Q-1, Q-2** and **Q-3** (4.7:1). A possible reason is that the higher reduction potential of **Q-4⊂C-1** promotes a longer lifetime of the radical cation product, thereby promoting more facile interconversion between *exo* and *endo* isomers *via* the uncyclized distonic radical cation intermediate. While dihalogenated quinones (**Q-5**, **Q-6** and **Q-7**) still showed some latent activity (Table 1, entries 9–11), this was lost altogether with chloroquinone (**Q-8**) and the anthraquinone derivatives, **Q-9** and **Q-10** (Table 1, entry 12). All quinones were catalytically inactive on their own.

Table 1. Quinone⊂C-1 catalyzed [4+2] cycloaddition of *trans*-anethole and cyclopentadiene.

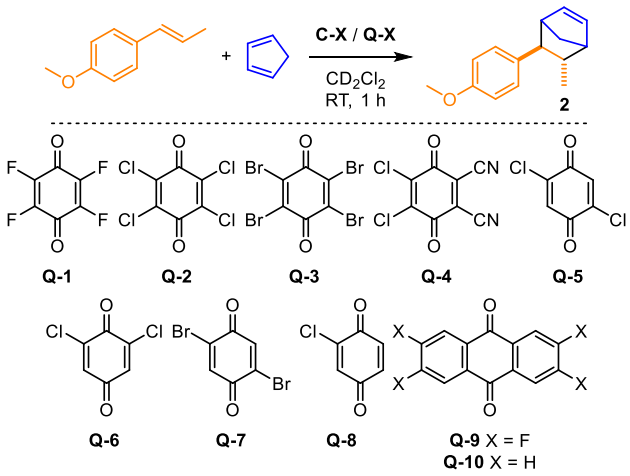

Entry	Cage	Quinone	Yield[a]
1	**C-1**	**Q-1**	99
2	**C-1**	–	0
3	–	**Q-1**	0
4[b]	**C-1**	**Q-1**	0
5	**C-2**	**Q-1**	0
6	**C-1**	**Q-2**	96
7	**C-1**	**Q-3**	99
8	**C-1**	**Q-4**	94
9	**C-1**	**Q-5**	5 (22)
10	**C-1**	**Q-6**	5 (22)
11	**C-1**	**Q-7**	4 (16)
12	**C-1**	**Q-8–10**	0

[a]Cage / quinone 0.5 mM, *trans*-anethole 10 mM, 20 mM cyclopentadiene; yield at 1 hour determined by ^{1}H NMR spectroscopy (values in parentheses at 24 hours). [b]With 20 mM **Q-10**.

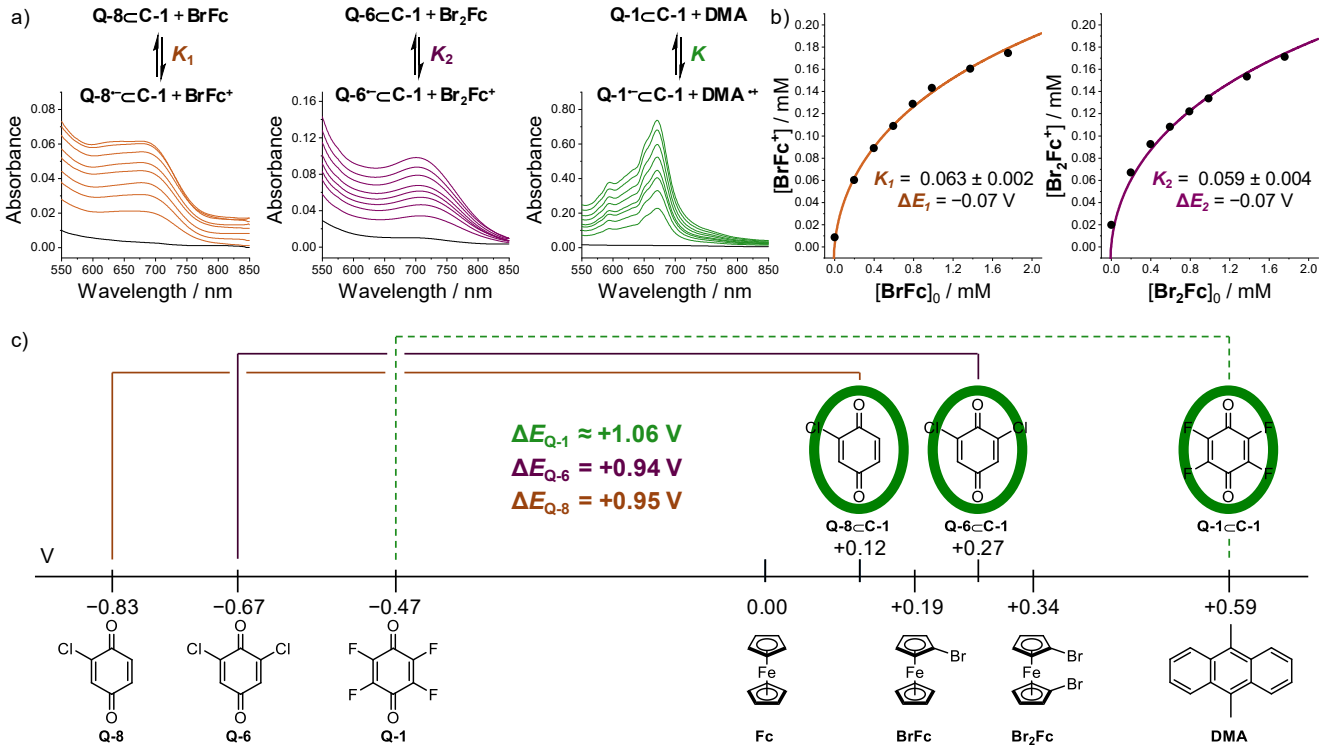

Figure 1. Quinone⊂**C-1** ET was investigated by (a) measuring the formation of oxidized species (bromoferrocinium (**BrFc**$^+$), dibromoferrocinium (**Br$_2$Fc**$^+$) and the dimethylanthracene radical cation (**DMA**$^{\bullet+}$)) using UV/Vis spectroscopy following addition of single electron donors (**BrFc**, **Br$_2$Fc** and **DMA**) to quinone⊂**C-1** complexes. The redox potentials for **Q-8⊂C-1** and **Q-6⊂C-1** were determined by (b) fitting these titrations to give ET equilibrium constants K and thereby ΔE with respect to the redox potentials of **Br$_2$Fc** and **BrFc**. (c) A comparison of the quinone⊂**C-1** redox potentials with respect to the free quinone, substrate and ferrocene reference compounds obtained by either quantitative analysis (orange and purple solid lines) or using qualitative observations based on catalyses and UV/Vis spectroscopy (green dashed line). The redox potentials of all non-cage compounds were measured by CV using a CH_2Cl_2 / NBu_4BArF electrolyte solution.

Perhaps surprisingly, the highly homologous cage **C-2** does not elicit redox catalysis for either the [4+2] cycloaddition of *trans*-anethole and cyclopentadiene (Table 1, entry 5) nor the [2+2] reaction of *trans*-anethole only. The poor [4+2] reactivity is partly explained because **C-2** rapidly catalyzes the thermal DA reaction of **Q-1** and cyclopentadiene. However, this does not explain the inactivity towards the [2+2] reaction, and hence the lack of redox reactivity more generally. This fundamental disparity likely stems from the different affinities of the two cages for anionic guests,[12] and by extension differing stabilization of the semiquinone radical anion **Q-1**$^{\bullet-}$. While we have been unable to measure absolute anion association constants for **C-1** and **C-2**, a competitive binding experiment with the triflate anion shows complete selectivity for **C-1** (see Figure S9). Further ET experiments with **C-2** show that redox modulation is not switched off altogether rather it is significantly reduced (see below).

Expanding the number of cycloaddition reactions, cyclohexadiene and isoprene also react with *trans*-anethole in the presence of 5 mol% **C-1**/**Q-1** (Scheme 2a), giving **3** and **4** in close to quantitative yield. For the reaction of *trans*-anethole and isoprene to give **4**, we have explored the possibility of reducing the catalyst loading further; it can be dropped to 1 mol% **C-1** (with 10 mol% **Q-1**) with only a slight drop in yield (see Table S1). This is a possible consequence of chain propagation[10b] caused by effective charge separation between the radical cation intermediate and the reduced yet cationic host-guest complex. *trans*-Anethole can also be replaced by *N*-methylvinyl carbazole[9d] (Scheme 2a), giving [4+2] products **5** and **6,** also in excellent yields. As previously noted, [2+2] formation of the head-to-head homodimer **1** using **Q-1⊂C-1** gave a modest yield. The homo-dimeric product of *N*-methylvinyl carbazole, **7**, can also be accessed in similar yields, yet interestingly, the cross [2+2] product of *trans*-anethole and *N*-methylvinyl carbazole gives product **8** in a much higher 77% yield (Scheme 2a). The hetero [2+2] cycloaddations of *trans*-anethole with electron neutral enes have also been carried out, giving cyclobutane adducts, **9**–**11**.

In addition to enes, **Q-1⊂C-1** also promotes the reaction of the electron rich diene, 9,10-dimethylanthracene (**DMA**), which undergoes [4+2] cycloaddition with *tert*-butyl benzoquinone (Scheme 2c). This reaction is complementary to the other [4+2] reactions reported above as it expands the scope to electron deficient enones. It is important to note that we have previously shown that *tert*-butyl benzoquinone is not a guest for these Pd_2L_4 cages. Also, **DMA** is too bulky to ingress and participate in a thermal DA reaction within the cavity,[2h] suggesting that ET can take place without substrate encapsulation. We also note that this reaction occurs readily in the absence of light suggesting that the mechanism does not involve photoinduced ET to the host guest complex. The use of **Q-4** in place of **Q-1** enhances the oxidizable substrate scope further. This is evidenced by reaction of cyclohexadiene with **Q-4⊂C-1**, which generates the [4+2] unsymmetrical dimer **12** (Scheme 2d).[13] In contrast, **Q-1⊂C-1** does not show any reactivity with cyclohexadiene.

Attempts to directly assess the redox potentials of the encapsulated quinone using cyclic voltammetry (CV) have proved incon-

clusive due to difficulties in detecting quinone/quinone$^{\bullet-}$⊂**C-1**. Instead we have measured several free quinones, substrate and reference compounds using 0.1 M NBu_4BArF in CH_2Cl_2 as electrolyte. This best represents the catalytic conditions, which uses the BArF salt of the cage in CH_2Cl_2 (see Supporting Information, section 11). **Q-1⊂C-1** can oxidise both the substrate **DMA** and reference compound tris(*p*-bromophenyl)amine (the reduced form of the Ledwith-Weitz salt) as directly evidenced by the formation of known[8,14] oxidized products using UV/Vis spectroscopy (Figure 1(a) and Figure S44). A comparison of the redox potentials of **DMA** ($E_{1/2}$ = 0.59 V vs Fc^+/Fc) and free **Q-1** ($E_{1/2}$ = −0.47 V vs Fc^+/Fc) indicates that **C-1** must shift the quinone redox potential anodically in excess of 1 V (Figure 1(c), dashed green line). Calculations show that the added electron is centered on the bound quinone and is thus stabilized by multiple non-covalent interactions (Figure S57).[15] We also note that **Q-1⊂C-2** is unable to oxidise either **DMA** or reference compound tris(*p*-bromophenyl)amine (Figure S44-45), in line with the lack of catalytic activity. However, ET is observed with ferrocene (Figure S46) showing the **C-2** can shift the redox potential of **Q-1**, albeit much less.

Further attempts to quantify the ET for the catalytic **Q-1⊂C-1** have been hampered by the limited stability of the **DMA** radical cation. Similarly, the *in situ* generated BArF equivalent of the Ledwith-Weitz salt showed similar instability, preventing quantitative analysis of **Q-1⊂C-1**. Instead, we have investigated the ET of less oxidizing host guest complexes **Q-6⊂C-1** and **Q-8⊂C-1** using more weakly reducing bromoferrocene (**BrFc**) and 1,1′-dibromoferrocene (**Br_2Fc**) reference compounds (Figures 1(a)). The resultant ferroconium BArF salts are stable in solution and their extinction coefficients are known.[8] Fitting this titration data (Figure 1(b), see Supporting Information for details) yielded ET equilibrium values (K) from which the redox potentials of the quinone⊂**C-1** host guest complexes have be calculated using the absolute values for **BrFc** ($E_{1/2}$ = 0.19 V vs Fc^+/Fc) and **Br_2Fc** ($E_{1/2}$ = 0.34 V vs Fc^+/Fc). Comparing the calculated redox potentials of **Q-6⊂C-1** ($E_{1/2}$ = 0.27 V vs Fc^+/Fc) and **Q-8⊂C-1** ($E_{1/2}$ = 0.12 V vs Fc^+/Fc) to the unbound **Q-6** ($E_{1/2}$ = −0.67 V vs Fc^+/Fc) and unbound **Q-8** ($E_{1/2}$ = −0.83 V vs Fc^+/Fc) respectively reveal an almost identical shift ($\Delta E_{1/2}$ = 0.94 and 0.95 V) for two separate titrations with different host-guest and reference compounds (Figure 1(c), purple and orange lines). These encapsulation-induced anodic shifts are also consistent with the ≈ 1.06 V that separates **DMA** and **Q-1**, suggesting that the cage shifts the quinone redox potential by a roughly uniform amount. These redox shifting properties of **C-1** compare favourably with the ~0.6 V anodic shift of *o*-quinone reduction potentials observed by Nocera and Jacobsen using small molecule, cationic H-bond donors.[8]

In conclusion, we have demonstrated a novel mode of cage catalysis that involves dramatically enhancing the oxidation power of commercially available quinones. Furthermore, encapsulation prevents further oxidation of the semiquinone, facilitating non-confined reactivity involving radical cation species. These results pave the way to other forms of non-confined catalysis wherein encapsulation triggers the release of reactive species from benign and easy to handle starting reagents.

ASSOCIATED CONTENT

Supporting Information

The Supporting Information is available free of charge on the ACS Publications website. This includes details of all catalytic experiments, substrate synthesis, host-guest titrations, redox and cyclic voltammetry experimental experiments, and computational procedures.

AUTHOR INFORMATION

Corresponding Author

Paul.Lusby@ed.ac.uk
Mark.Symes@glasgow.ac.uk
Fernanda.duartegonzalez@chem.ox.ac.uk

Notes

The authors declare no competing financial interests.

ACKNOWLEDGMENT

We acknowledge the following EPSRC Centers for Doctoral training: Critical Resource Catalysis (CRITICAT, EP/L016419/1) for a studentship for RLS, and Theory and Modelling in Chemical Sciences (EP/L015722/1) for a studentship to TAY generously supported by AWE. MDS thanks the Royal Society for a University Research Fellowship (UF150104).
The authors acknowledge the use of the EPSRC Tier-2 National HPC Facility Service Cirrus (www.cirrus.ac.uk).

REFERENCES

(1) Pauling, L. Nature of Forces between Large Molecules of Biological Interest**.** *Nature* **1948**, *161*, 707.
(2) (a) Rideout, D. C.; Breslow, R. Hydrophobic acceleration of Diels-Alder reactions**.** *J. Am. Chem. Soc.* **1980**, *102*, 7817. (b) Kang, J.; Rebek Jr., J. Acceleration of a Diels–Alder reaction by a self-assembled molecular capsule**.** *Nature* **1997**, *385*, 50; (c) Yoshizawa, M.; Tamura, M.; Fujita, M. Diels-alder in aqueous molecular hosts: unusual regioselectivity and efficient catalysis. *Science* **2006**, *312*, 251; (d) Fiedler, D.; Bergman, R. G.; Raymond, K. N. Supramolecular catalysis of a unimolecular transformation: aza-Cope rearrangement within a self-assembled host. *Angew. Chem. Int. Ed*. **2004**, *43*, 6748. (e) Samanta, D.; Mukherjee, S.; Patil, Y. P.; Mukherjee, P. S. Self-Assembled Pd_6 Open Cage with Triimidazole Walls and the Use of Its Confined Nanospace for Catalytic Knoevenagel- and Diels–Alder Reactions in Aqueous Medium. *Chem. Eur. J.* **2012**, *18*, 12322. (f) Bolliger, J. L.; Belenguer, A. M.; Nitschke, J. R. Enantiopure water-soluble [Fe_4L_6] cages: host-guest chemistry and catalytic activity. *Angew. Chem. Int. Ed.* **2013**, *52*, 7958. (g) Cullen, W.; Misuraca, M. C.; Hunter, C. A.; Williams, N. H.; M. D. Ward. Highly efficient catalysis of the Kemp elimination in the cavity of a cubic coordination cage. *Nat. Chem.* **2016**, *8*, 231. (h) Martí-Centelles, V.; Lawrence, A. L.; Lusby, P. J., High Activity and Efficient Turnover by a Simple, Self-Assembled "Artificial Diels–Alderase". *J. Am. Chem. Soc.* **2018,** *140*, 2862 (i) Holloway, L. R.; Bogie, P. M.; Y. Lyon, Y.; Ngai, C.; Miller, T. F.; Julian, R. R.; Hooley, R. J. Tandem Reactivity of a Self-Assembled Cage Catalyst with Endohedral Acid Groups. *J. Am. Chem. Soc.* **2018**, *140*, 26.
(3) (a) Merlau, M. L.; del Pilar Mejia, M.; Nguyen, S. T.; J. T. Hupp. Artificial Enzymes Formed through Directed Assembly of Molecular Square Encapsulated Epoxidation Catalysts. *Angew. Chem. Int. Ed.* **2001**, *40*, 4239. (b) Slagt, V. F.; Reek, J. N. H.; Kamer, P. C. J.; van Leeuwen, P. W. N. M. Assembly of Encapsulated Transition Metal Catalysts. *Angew. Chem. Int. Ed.* **2001**, *40*, 4271. (c) Wang, Q.-Q.; Gonell, S.; Leenders, S. H. A. M.; Dürr, M.; Ivanović-Burmazović, I.; Reek, J. N. H. Self-assembled nanospheres with multiple endohedral binding sites pre-organize catalysts and substrates for highly efficient reactions. *Nat. Chem.* **2016**, *8*, 225. (d) Nurttila, S. S.; Brenner, W.; Mosquera, J.; van Vliet, K. M.; Nitschke, J. R.; Reek, J. N. H. Size-Selective Hydroformylation by a Rhodium Catalyst Confined in a Supramolecular Cage. *Chem. Eur. J.* **2019**, *25*, 609.
(4) (a) Wang, Z. J.; Brown, C. J.; Bergman, R. G.; Raymond, K.N.; Toste, F. D. Hydroalkoxylation Catalyzed by a Gold(I) Complex Encapsulated in a Supramolecular Host. *J. Am. Chem. Soc*. **2011**, *133*, 7358 (b) Brown, C. J.; Miller, G. M.; Johnson, M. W.; Bergman, R. G.; Raymond K. N. High-Turnover Supramolecular Catalysis by a Protected Ruthenium(II) Complex in Aqueous Solution. *J. Am. Chem. Soc.* **2011**, *133*, 11964. (c) Kaphan, D. M.; Levin, M. D.; Bergman, R. G.; Raymond, K. N.; Toste, F. D. A supramolecular microenvironment strategy for transition metal catalysis. *Science* **2015**, *350*, 1235. (d) Bender, T.A.; Bergman, R.G.; Raymond, K.N.; Toste, F.D. A Supramolecular Strategy for Selective Catalytic Hydrogenation Independent of Remote Chain Length. *J. Am. Chem. Soc.* **2019**, 141, 11806.
(5) (a) Sun, W.-Y.; Kusukawa, T.; Fujita, M. Electrochemically Driven Clathration/Declathration of Ferrocene and Its Derivatives by a Nanometer-

Sized Coordination Cage. *J. Am. Chem. Soc.* **2002**, *124*, 11570. (b) Yoshizawa, M.; Kumazawa, K.; Fujita, M. Room-Temperature and Solution-State Observation of the Mixed-Valence Cation Radical Dimer of Tetrathiafulvalene, $[(TTF)_2]^{+\bullet}$, within a Self-Assembled Cage. *J. Am. Chem. Soc.* **2005**, *127*, 13456. (c) He, Q.-T.; Li, X.-P.; Liu, Y.; Yu, Z.-Q.; Wang, W.; Su, C.-Y.; Copper(I) Cuboctahedral Coordination Cages: Host–Guest Dependent Redox Activity. *Angew. Chem. Int. Ed.* **2009**, *48*, 6156. (d) Furutani, Y.; Kandori, H.; Kawano, M.; Nakabayashi, K.; Yoshizawa, M.; Fujita, M. In Situ Spectroscopic, Electrochemical, and Theoretical Studies of the Photoinduced Host−Guest Electron Transfer that Precedes Unusual Host-Mediated Alkane Photooxidation. *J. Am. Chem. Soc.* **2009**, *131*, 4764. (e) Gera R.; Das, A.; Jha, A.; Dasgupta, J. Light-Induced Proton-Coupled Electron Transfer Inside a Nanocage. *J. Am. Chem. Soc.* **2014**, *136*, 15909. (f) Rizzuto, F. J.; Wood, D. M.; Ronson, T. K.; Nitschke, J. R. Tuning the Redox Properties of Fullerene Clusters within a Metal−Organic Capsule. *J. Am. Chem. Soc.* **2017**, *139*, 11008. (g) Matsumoto, K.; Kusaba, S.; Tanaka, Y.; Sei, Y.; Akita, M.; Aritani, K.; Haga, M.; Yoshizawa, M. A Peanut-Shaped Polyaromatic Capsule: Solvent-Dependent Transformation and Electronic Properties of a Non-Contacted Fullerene Dimer. *Angew. Chem. Int. Ed.* **2019**, *58*, 8463.

(6) (a) Dalton, D. M.; Ellis, S. R.; Nichols, E. M.; Mathies, R. A.; Toste, F. D.; Bergman, R. G.; Raymond, K. N. Supramolecular $Ga_4L_6^{12-}$ Cage Photosensitizes 1,3-Rearrangement of Encapsulated Guest via Photoinduced Electron Transfer. *J. Am. Chem. Soc.* **2015**, *137*, 10128. (b) Jing, X.; He, C.; Yang, Y.; Duan, C. A Metal–Organic Tetrahedron as a Redox Vehicle to Encapsulate Organic Dyes for Photocatalytic Proton Reduction. *J. Am. Chem. Soc.* **2015**, *137*, 3967. (c) Cai, L.-X.; Li, S.-C.; Yan, D.-N.; Zhou, L.-P.; Guo, F.; Sun, Q.-F. Water-Soluble Redox-Active Cage Hosting Polyoxometalates for Selective Desulfurization Catalysis. *J. Am. Chem. Soc.* **2018**, *140*, 4869. (d) Lu, Z.; Lavendomme, R.; Burghaus, O.; Nitschke, J. R. A Zn_4L_6 Capsule with Enhanced Catalytic C—C Bond Formation Activity upon C_{60} Binding. *Angew. Chem. Int. Ed.* **2019**, *58*, 9073. (e) Nurttila, S. S.; Zaffaroni, R.; Mathew, S.; Reek, J. N. H. Control of the overpotential of a [FeFe] hydrogenase mimic by a synthetic second coordination sphere *Chem. Commun.,* **2019**, *55*, 3081. (f) Wu, K.; Li, K.; Chen, S.; Hou, Y.-J.; Lu, Y.-L.; Wang, J.-S.; Wei, M.-J.; Pan, M.; Su, C.-Y. The Redox Coupling Effect in a Photocatalytic Ru^{II}-Pd^{II} Cage with TTF Guest as Electron Relay Mediator for Visible-Light Hydrogen-Evolving Promotion. *Angew. Chem. Int. Ed.* **2019**. 10.1002/anie.201913303.

(7) (a) August, D. P.; Nichol, G. S.; Lusby, P. J. Maximizing Coordination Capsule–Guest Polar Interactions in Apolar Solvents Reveals Significant Binding *Angew. Chem. Int. Ed.* **2016**, 55, 15022. (b) Young, T. A.; Martí-Centelles, V.; Wang, J.; Lusby, P. J; Duarte, Fernanda Rationalizing the Activity of an "Artificial Diels-Alderase": Establishing Efficient and Accurate Protocols for Calculating Supramolecular Catalysis. *J. Am. Chem. Soc.* **2019**, DOI:10.1021/jacs.9b10302,

(8) Turek, A. K.; Hardee, D. J.; Ullman, A. M.; Nocera, D. G.; Jacobsen, E. N. Activation of Electron-Deficient Quinones through Hydrogen-Bond-Donor-Coupled Electron Transfer. *Angew. Chem. Int. Ed.* **2016**, *55*, 539.

(9) (a) Bauld, N. L.; Pabon, R. Cation Radical Catalyzed Olefin Cyclodimerization. *J. Am. Chem. Soc.* **1983**, *105*, 5158. (b) Pabon, R, A.; Bellville, D. J.;. Bauld, N. L Cation Radical Diels-Alder Reactions of Electron-Rich Dienophiles. *J. Am. Chem. Soc.* **1983**, *105*, 5158. (c) Bauld, N. L.; Gao, D. Approaching a possible stepwise/concerted mechanistic crossover point in the cation radical cycloadditions of *cis*- and *trans*-anethole. *J. Chem. Soc*., *Perkin Trans. 2* **2000**, 931. (d) Bauld, N. L.; Gao, D. *N*-(trans-1-Propenyl)carbazole: an excellent dienophile for cation radical Diels–Alder cycloadditions. *Tetrahedron Lett.* **2000**, *41*, 5997.

(10) (a) Ischay, M. A.; Ament, M. S.; Yoon, T. P. Crossed intermolecular [2 + 2] cycloaddition of styrenes by visible light photocatalysis. *Chem. Sci.*, **2012**, 3, 2807. (b) Lin, S.; Ischay, M. A.; Fry, C. G.; Yoon, T. P. Radical Cation Diels–Alder Cycloadditions by Visible Light Photocatalysis. *J. Am. Chem. Soc.* **2011**, *133*, 19350.

(11) Huynh, M. T.; Anson, C. W.; Cavell, A. C.; Stahl, S. S.; Hammes-Schiffer, S. Quinone 1 e^- and 2 e^-/2 H^+ Reduction Potentials: Identification and Analysis of Deviations from Systematic Scaling Relationships. *J. Am. Chem. Soc.* **2016**, *138*, 15903.

(12) Lewis, J. E.M.; Crowley, J. D. Exo- and endohedral interactions of counteranions with tetracationic Pd_2L_4 metallosupramolecular architectures. *Supramol. Chem.* **2014**, *26*, 173.

(13) The half-wave reduction potentials (vs SCE, CH_3CN, irreversible) of *trans*-anethole and 1,3-cyclohexadiene are +1.11 V and +1.53 V, respectively, see Bauld, N. L.; Harirchian, B.; Reynolds, D. W.; White, J. C. A Strategy for Intermolecular Diels-Alder Cycloaddition to Enamides. *J. Am. Chem. Soc.* **1988**, *110*, 8111. Attempts to record the CVs of these substrates in CH_2Cl_2 using NBu_4BArF electrolyte to best represent catalytic conditions showed ill-defined waves (see Figures S41 and S43).

(14) Rathore, R.; Kochi, J. K.; Canavesi, A.; Miller, L. L.; Sebastiani, G. V.; Francis, G. W.; Szúnyog, J.; Långström, B. Acid Catalysis vs. Electron-Transfer Catalysis via Organic Cations or Cation-Radicals as the Reactive Intermediate. Are These Distinctive Mechanisms? *Acta Chem. Scand.* **1998**, *52*, 114.

(15) (a) Zhao, Y.; Truhlar, D. G., The M06 Suite of Density Functionals for Main Group Thermochemistry, Thermochemical Kinetics, Noncovalent Interactions, Excited States, and Transition Elements: Two New Functionals and Systematic Testing of Gour M06-class Functionals and 12 other Functionals. *Theor. Chem. Acc.* **2008,** 120, 215.; (b) Weigend, F.; Ahlrichs, R., Balanced Basis Sets of Split Valence, Triple Zeta Valence and Quadruple Zeta Valence Quality for H to Rn: Design and Assessment of Accuracy. *Phys. Chem. Chem. Phys.* **2005,** 7, 3297; (c) Marenich, A. V.; Cramer, C. J.; Truhlar, D. G., Universal Solvation Model Based on Solute Electron Density and on a Continuum Model of the Solvent Defined by the Bulk Dielectric Constant and Atomic Surface Tensions. *J. Phys. Chem. B* **2009,** 113, 6378; (d) Toward reliable density functional methods without adjustable parameters: The PBE0 model. *J. Chem. Phys.* **1999,** 110, 6158; (e) S. Grimme, S. Ehrlich and L. Goerigk, Effect of the damping function in dispersion corrected density functional theory, *J. Comp. Chem*. **2011**, 3, 1456-1465.

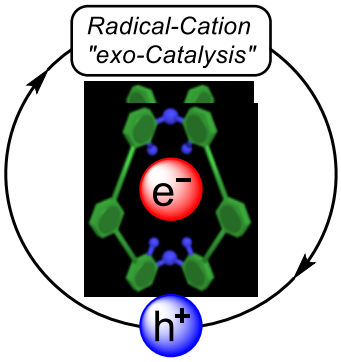
Radical-Cation
"exo-Catalysis"
e⁻
h⁺